High-spin states in ^{156}Yb and structure evolutions at large angular momenta in even-A Yb isotopes

Z. Y. Li, H. Hua,* S. Y. Wang,† J. Meng, Z. H. Li, X. Q. Li, F. R. Xu, H. L. Liu, S. Q. Zhang, Y. L. Ye, D. X. Jiang, T. Zheng, L. Y. Ma, F. Lu, F. Y. Fan, L. Y. Han, H. Wang, J. Xiao, D. Chen, X. Fang, and J. L. Lou
School of Physics and State Key Laboratory of Nuclear Physics and Technology, Peking University, Beijing 100871, People's Republic of China

S. G. Zhou
Institute of Theoretical Physics, Chinese Academy of Sciences, Beijing 100080, People's Republic of China and Center of Theoretical Nuclear Physics, National Laboratory of Heavy Ion Accelerator, Lanzhou 730000, People's Republic of China

L. H. Zhu, X. G. Wu, G. S. Li, C. Y. He, Y. Liu, X. Q. Li, X. Hao, B. Pan, and L. H. Li
China Institute of Atomic Energy, Beijing 102413, People's Republic of China
(Received 14 March 2008; published 30 June 2008)

High-spin states of ^{156}Yb have been studied via the ^{144}Sm(^{16}O,4n)^{156}Yb fusion-evaporation reaction at beam energy 102 MeV. The positive-parity yrast band and negative-parity cascade have been extended up to higher-spin states, respectively. In the present work, the negative-parity sequence above the 25^- state was found to be irregular and fragment into many parallel branches. This pattern may related to the excitation from the nucleon in the $Z = 64$, $N = 82$ core. The characteristics of alignment plot and E-GOS curve for the positive-parity yrast sequence in ^{156}Yb indicate that this nucleus may undergo an evolution from quasivibrational to quasirotational structure with increasing angular momentum. Based on a systematic summary of the available experimental alignments for the even-A ^{156,158,160,162,164}Yb isotopes, the structural evolutions induced by the increase in angular momentum, as well as by the change in neutron numbers, in these even-A Yb isotopes have been discussed in comparison with the cranked Woods-Saxon-Strutinsky calculations by means of total-Routhian-surface (TRS) methods.

DOI: 10.1103/PhysRevC.77.064323 PACS number(s): 23.20.Lv, 21.10.Re, 25.70.Gh, 27.70.+q

I. INTRODUCTION

The light rare-earth nuclei around $A = 150$ mass region, which locate above the double-closed shells $N = 82$ and $Z = 64$, have attracted a lot of experimental and theoretical studies. For example, these experimental studies led to the identification of many interesting phenomena: the pronounced vibrational nature of the low-lying members of the ground state band [1–4]; the occurrence of an island of long-lived isomers [5,6]; the superdeformed nuclear shape with a major-to-minor axis ratio of approximately 2 [7,8]; the shape transition from prolate collective to oblate noncollective rotation via the mechanism of band termination between spins $I \sim 30$–42 [9,11]. At the same time, theoretical studies of the nuclear structure properties over a wide range of isospin, not only for the ground states [12–14] but also for the low and high-spin states [15–17], have been made to try to understand systematically the microscopic origin of these rich phenomena.

The excitation-energy systematics of the low-lying states in these mass region nuclei are plotted in Fig. 1. It shows that with increasing neutron number, the nuclear deformations increase and the nuclear collective modes of motion for the low-lying states of the ground state bands change from vibrational behavior to rotational behavior. The nuclei situated in the transitional region between spherical and deformed nuclei were found to have rather soft potential-energy surface. Their internal structures are susceptible to the increased angular momentum, especially the alignment of a high-j intruder nucleon pair. Rich band crossing phenomena has been observed in this mass region, where the alignments of the $\nu i_{13/2}$, $\nu h_{9/2}$, and $\pi h_{11/2}$ pairs were suggested to play important roles. Their critical alignment frequencies were found to be close to each other and the relatively small shifts in alignment frequencies can replace one alignment by another, which will produce large differences in the band behavior and intrinsic structure [18]. Thus, study of the properties of these nuclei at high-spin states serves as an important test for various theoretical models. Here, we report a study of high-spin states in ^{156}Yb, which are populated by the ^{144}Sm(^{16}O,4n)^{156}Yb fusion-evaporation reaction. Its level scheme was compared with similar structures observed in the neighboring $N = 86$ isotones. To get an overall picture of the alignments and more insight for the structure changes caused by these alignments in the even-A Yb isotopes, a systematic summary of the available experimental alignments has been given for these nuclei with a comparison to the cranked Woods-Saxon-Strutinsky calculations by means of total-Routhian-surface (TRS) methods.

II. EXPERIMENT

The present experiment was performed at the HI-13 tandem facility of the China Institute of Atomic Energy (CIAE).

*Hhua@hep.pku.edu.cn
†present address: Department of Space Science and Applied physics, shandong university at Weihai, Weihai 264209, People's Republic of china.

 ©2008 The American Physical Society

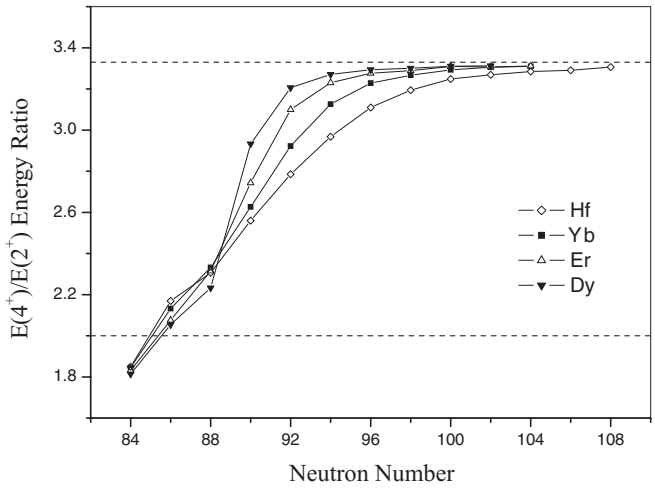

FIG. 1. Systematics of the E_{4^+}/E_{2^+} energy ratios as a function of neutron number in the Dy, Er, Yb, and Hf isotopes. The theoretical value of E_{4^+}/E_{2^+} for a harmonic vibrator is 2.00, and for a rigid rotor is 3.33.

The ^{144}Sm(^{16}O,4n)^{156}Yb reaction was used to populate the high-spin states in ^{156}Yb. The target was ^{144}Sm with a thickness of 1.2 mg/cm^2. The reaction products recoiled into vacuum. The deexcitation γ rays were detected by an γ detector array which consists of 12 high-purity germanium (HPGe) detectors with BGO anti-Compton suppressors and two planar high-purity germanium (HPGe) detectors. The energy resolutions of these detectors were 2.0–3.0 keV at 1.33 MeV. All detectors were calibrated using the standard ^{152}Eu and ^{133}Ba γ-ray sources. In order to determine the optimum beam energy for producing ^{156}Yb, γ-rays excitation functions were measured using beam energies of 96, 100, 102, 104, 108, 111 MeV. The total projection spectra obtained from the γ-γ coincidence data at beam energy 96, 102, 108 MeV are shown in Fig. 2. Through comparing with the PACE4 program calculations, the beam energy of 102 MeV was chosen to be suitable for producing ^{156}Yb relative to other neighboring nuclei.

A total of 2.2 $\times$ 10^8 coincident events were collected, from which a symmetric γ-γ matrix was built. The level scheme analysis was performed using the RADWARE program [19]. The γ-ray spectra gated on the known γ-ray transitions in ^{156}Yb are shown in Fig. 3. The peaks were broader due to Doppler effects from the recoiling nuclei and the gains of the spectra at different angles have been corrected to compensate for the Doppler shift of γ rays. In order to obtain the Directional Correlations of γ rays deexciting Oriented states (DCO) intensity ratios to determine the multipolarities of γ-ray transitions, the detectors around 90° with respect to the beam direction were sorted against the detectors around 40° to produce a two-dimensional angular correlation matrix. In general, stretched quadrupole transitions were adopted if DCO ratios were larger than 1.0, and stretched dipole transitions were assumed if DCO ratios were less than 0.8.

III. RESULTS AND DISCUSSION

The spectroscopy of ^{156}Yb has been previously studied via ^{144}Sm(^{16}O,4n)^{156}Yb reaction by the Lister *et al.* [2]. The partial level scheme of ^{156}Yb, deduced from the present work is shown in Fig. 4. It was constructed from γ-γ coincidence relationships, intensity balances and DCO analyses. The results are summarized in Table I. In the earlier study [2], the yrast even-spin positive-parity cascade in ^{156}Yb was established up to spin 10$^+$ at 2956 keV and one γ-ray transition of 614.5 keV was tentatively assigned to the positive-parity sequence due to its too weak intensity. All these transitions were also observed by the present work. By requiring the coincidence with the known γ-ray transitions under spin 12$^+$ of the positive-parity cascade in ^{156}Yb, four new coincident γ-ray transitions of 520.3, 641.9, 731.9, and 733.3 keV were observed in the γ-ray spectra. The DCO ratio analyses suggest that γ-ray transitions of 520.3, 641.9, and 731.9 keV have quadrupole transition characters.

A $J^\pi = 11^-$ isomer has been observed in the $N = 86$ isotones [2,20–22]. They were found to have almost same

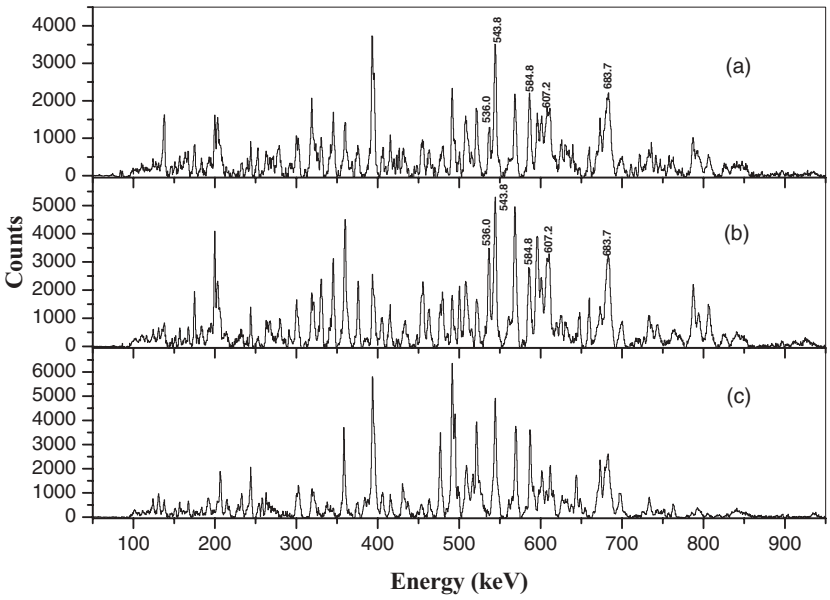

FIG. 2. Background-subtracted total projection spectra obtained from the γ-γ coincidence data at beam energy (a) 96 MeV; (b) 102 MeV; (c) 108 MeV. The labeled peaks correspond to known γ-ray transitions under spin 10$^+$ of the positive-parity cascade in ^{156}Yb. They contain contaminants from the neighboring Yb and Tm nuclei.

TABLE I. γ-ray energies, excitation energies, relative γ-ray intensities, and DCO ratios in ^{156}Yb.

E_γ (keV)	E_i (keV)	E_f (keV)	Int. (%)	DCO ratio	The γ-ray gate for DCO ratio (keV)	Assignment
71.8	3027.3	2955.5				$11^- \rightarrow 10^+$
156.2	8930.5	8774.3	2.4(0.1)	0.47(0.09)	375.4	$\lambda = 1$
184.1	7028.4	6844.3				
185.0	4974.2	4789.2				
290.0	5574.8	5284.8	3.3(0.1)			
310.6	5284.8	4974.2	3.7(0.2)			
315.0	4789.2	4474.2				
315.3	9245.8	8930.5				
370.4	7774.2	7403.8	1.5(0.3)	1.37(0.68)	375.4	$\lambda = 2$
375.4	7403.8	7028.4	15.4(2.0)	0.84(0.06)	646.8	$25^- \rightarrow 23^-$
405.3	8774.3	8369.0	3.5(0.3)	0.78(0.35)	375.4	$\lambda = 2$
500.0	4974.2	4474.2	27.1(0.7)	1.06(0.06)	787.8	$17^- \rightarrow 15^-$
520.3	4090.4	3570.1	7.4(0.2)	0.83(0.15)	614.6	$14^+ \rightarrow 12^+$
536.0	536.0	0	100	1.42(0.12)	607.2	$2^+ \rightarrow 0^+$
543.8	2271.8	1728.0	70.9(1.9)	2.22(0.15)	536.0	$8^+ \rightarrow 6^+$
584.8	1728.0	1143.2	88.9(3.4)	2.37(0.11)	536.0	$6^+ \rightarrow 4^+$
600.6	5574.8	4974.2	24.1(0.7)	1.20(0.22)	659.1	$19^- \rightarrow 17^-$
607.2	1143.2	536.0	95.4(4.1)	1.86(0.11)	536.0	$4^+ \rightarrow 2^+$
614.6	3570.1	2955.5	20.3(0.4)	1.40(0.18)	584.8	$12^+ \rightarrow 10^+$
622.7	6844.3	6221.6				
624.5	8028.3	7403.8	6.2(1.4)			
641.9	4732.3	4090.4	5.3(0.2)	0.85(0.16)	614.6	$16^+ \rightarrow 14^+$
646.8	6221.6	5574.8	23.2(0.9)	1.85(0.08)	659.1	$21^- \rightarrow 19^-$
659.1	4474.2	3815.1	34.6(0.6)	1.17(0.06)	787.8	$15^- \rightarrow 13^-$
683.7	2955.5	2271.8	62.4(5.9)	1.83(0.10)	607.2	$10^+ \rightarrow 8^+$
731.9	5464.2	4732.3	1.4(0.1)	0.94(0.67)	614.6	$18^+ \rightarrow 16^+$
733.3	6197.5	5464.2				$(20^+) \rightarrow 18^+$
787.8	3815.1	3027.3	37.1(0.9)	1.37(0.12)	543.8	$13^- \rightarrow 11^-$
806.8	7028.4	6221.6	18.1(0.3)	0.97(0.23)	646.8	$23^- \rightarrow 21^-$
923.1	8697.3	7774.2				
925.1	10231.9	9306.8				
965.2	8369.0	7403.8	5.7(0.5)			
1278.5	9306.8	8028.3	2.8(0.3)			

excitation energies. The small magnitude of the g factor of the isomeric state in ^{154}Er, measured by the Nguyen *et al.* [23] and Rafailovich *et al.* [24], respectively, suggested that the main configuration of its wave function is the two neutron quasiparticle excitation $\upsilon(i_{13/2}, h_{9/2})$. Built on the $J^\pi = 11^-$ isomer in ^{156}Yb, an odd-spin negative-parity cascade up to spins 25^- at 7405 keV was found in Ref. [2]. The level sequence exhibits neither a rotational character nor a vibrational character. In Ref. [2], four coincident γ-ray transitions were observed above the 25^- state, but they were not conclusively shown in mutual coincident spectra due to the too weak intensity. Thus, they were not assigned the spin and parity at that time. In the current study as shown in Fig. 4, above the 25^- state, the negative-parity sequence becomes irregular and fragments into several parallel branches. Except the four already known transitions, five new transitions of 370.4, 405.3, 923.1, 925.1, and 1278.5 keV were observed. In the present work, the transitions above the 25^- state are also too weak in intensity. According to the DCO values, only a quadrupole assignment were made for the transitions of 370.4 and 405.3 keV. No spins and parities are assigned to these states. The sequence of these transitions above the 25^- state follows the order of their relative intensities.

In Ref. [2], the neutron $\upsilon(f_{7/2}, h_{9/2}, i_{13/2})$ configurations were suggested to play a major role in the wave functions of the low-lying positive parity levels below 8^+ in ^{156}Yb, while only a small contribution may comes from the proton configurations. This argument was further supported in the following studies of low-lying states in the even-Z, $N = 86$ isotones [3,4]. According to the systematics [2,3,22] and theoretical calculations [22], the negative-parity states built on the isomeric 11^- state in ^{156}Yb are most likely due to the coupling $(\nu f_{7/2})^2(\pi h_{11/2})^2$ to the aligned $\upsilon(i_{13/2}h_{9/2})_{11}$-configuration of the 11^- isomer [2]. Above the 25^- state in ^{156}Yb, several parallel cascades were observed in the present work. Since the angular momentum of these states above the 25^- state in ^{156}Yb is close to the maximum angular momentum possible from alignment of the valence particles outside the $Z = 64$, $N = 82$ core, these parallel cascades above the 25^- state in ^{156}Yb may involve the excitation from nucleon in the

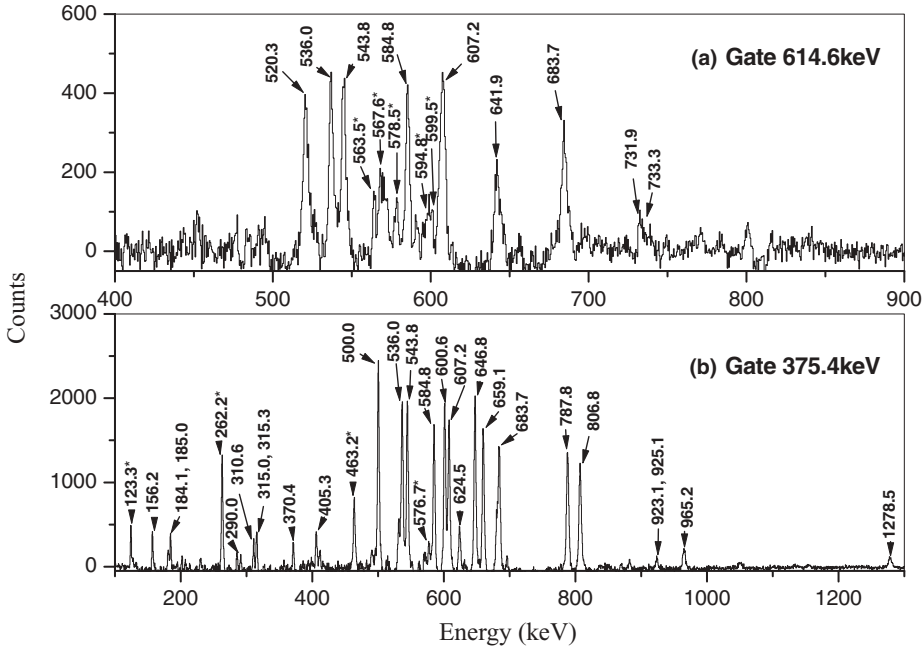

FIG. 3. Coincident γ-ray spectra with gating on (a) 614.6 keV transition; (b) 375.4 keV transition. The peaks marked star are known contaminants from the neighboring Tm and Yb nuclei.

$Z = 64$, $N = 82$ core. Similar phenomena was also observed in the high-spin structures of the neighboring $N = 86$ isotones ^{154}Er [22] and ^{158}Hf [3].

The systematic properties of the high positive-parity spin states in even-A Yb isotopes were studied by comparing the aligned spins as a function of rotational frequency. In

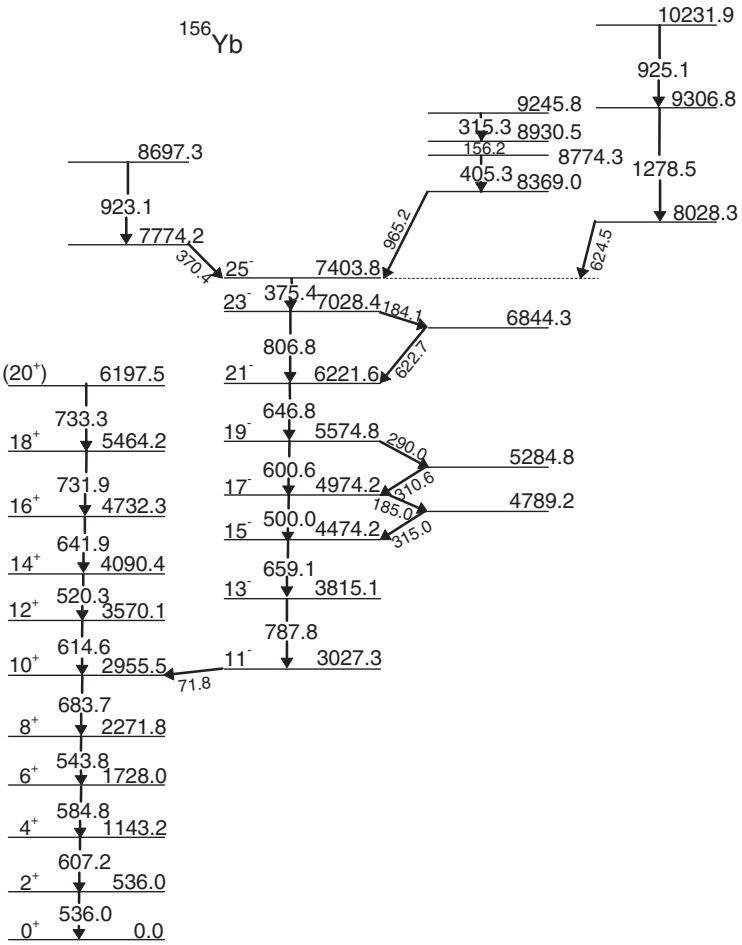

FIG. 4. Partial level scheme of ^{156}Yb. Energies are in keV.

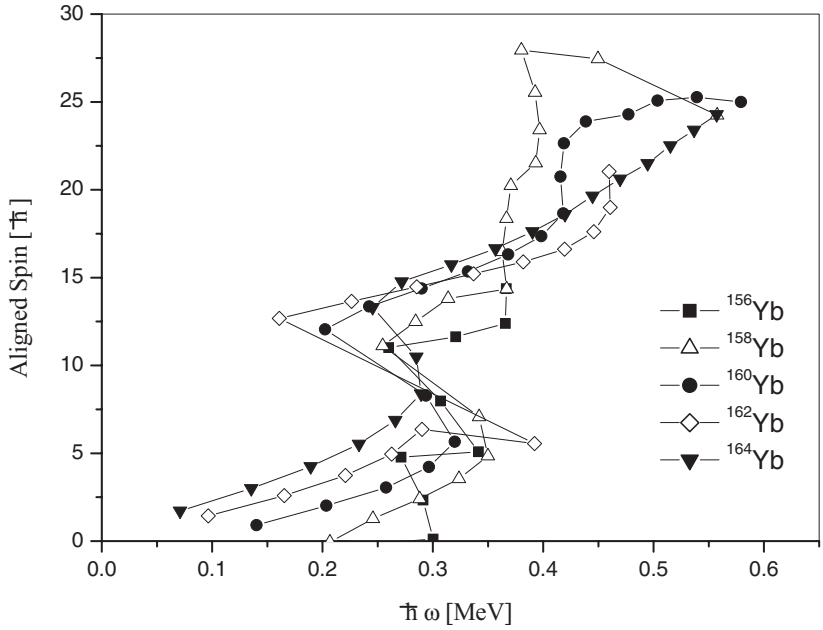

FIG. 5. Aligned spins as a function of the rotational frequency for the positive-parity yrast sequences in the even-A ^{156,158,160,162,164}Yb isotopes. Harris parameters of $J_0 = 10.0\hbar^2$/MeV and $J_1 = 50.0\hbar^4$/MeV^3 have been assumed.

Fig. 5, the experimental alignments for the positive-parity yrast sequences in the even-A Yb isotopes are ploted. In contrast to the well defined rotational yrast bands observed in ^{158,160,162,164}Yb, the collective mode of motion in ^{156}Yb may have characteristic that ranges between quasivibration and quasirotation. This evolution from quasivibrational to quasirotational structure as a function of spin is manifest in Fig. 6, where the ratio of $E_\gamma(I \to I-2)/I$ versus spin I is plotted, that is, the so-called E-GOS (E-Gamma Over Spin) curve [25]. For a vibrator, the value of this ratio gradually diminishes to zero as the spin increases, while for an axially symmetric rotor it approaches a constant, $4(\hbar^2/2J)$. Here J is the static moment of inertia. As shown in Fig. 6, the E-GOS value of ^{156}Yb evolves from an approximate hyperbolic locus expected for quasivibrational structure to a constant, which is very close to the E-GOS value of good rotor ^{164}Yb. Our TRS calculations, which is shown in Fig. 7 and will be discussed in the following, indicate that the soft quadrupole deformation $\beta_2(= 0.139)$ at ground state in ^{156}Yb will be stabilized with the alignment of a high-j intruder $h_{11/2}$ proton pair. This may account for the evolution from vibrational to rotational structure in ^{156}Yb.

As shown in Fig. 5, the first $i_{13/2}$ neutron band crossings in the ^{158,160,162,164}Yb isotopes occur around almost same rotational frequencies 0.27 MeV [10,18,26–28], although these nuclei have different quadrupole deformations [12–14]. The constant crossing frequency has been explained in term of the compensation between the decrease in the neutron pair gap and the decrease in the alignment of the $i_{13/2}$ neutron pair with increasing neutron number [29], while the sharpness

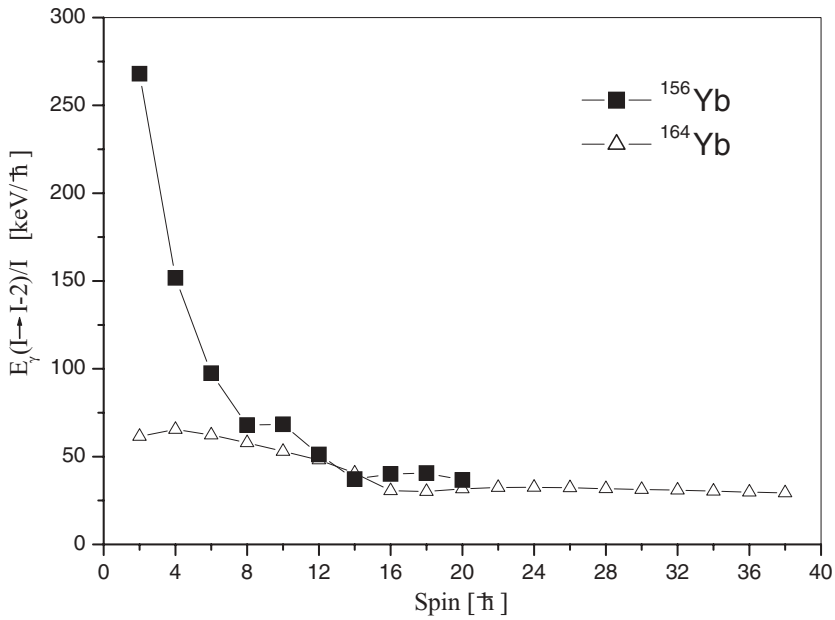

FIG. 6. E-GOS curves for the ^{156}Yb and ^{164}Yb.

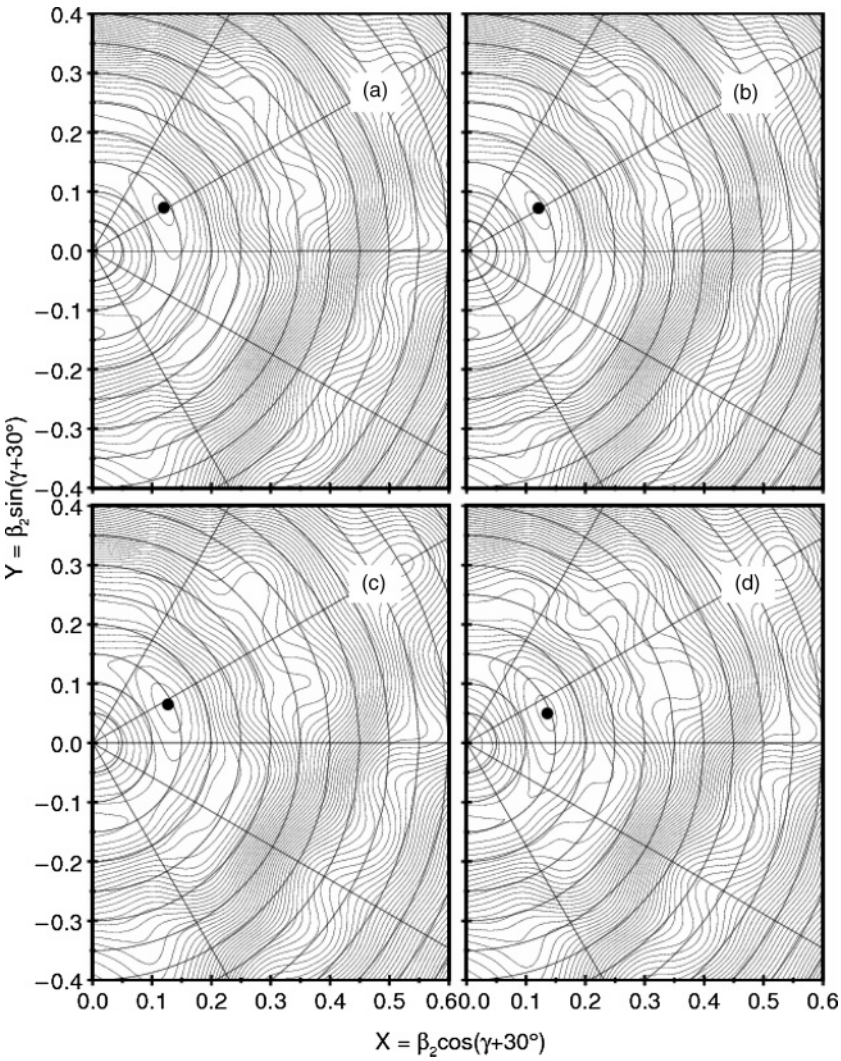

FIG. 7. TRS calculations for the yrast sequence in ^{156}Yb. The energy contours are at 200 keV intervals. The deformation parameters for the individual minima are (a) $\hbar\omega = 0.00$ MeV, $\beta_2 = 0.139$, $\gamma = 0.0^\circ$, and $\beta_4 = 0.028$; (b) $\hbar\omega = 0.05$ MeV, $\beta_2 = 0.139$, $\gamma = 0.0^\circ$, and $\beta_4 = 0.028$; (c) $\hbar\omega = 0.15$ MeV, $\beta_2 = 0.142$, $\gamma = -2.9^\circ$, and $\beta_4 = 0.030$; (d) $\hbar\omega = 0.25$ MeV, $\beta_2 = 0.145$, $\gamma = -9.8^\circ$, and $\beta_4 = 0.033$.

evolution of these first backbends observed in the Yb isotopes may correspond to the oscillations with neutron number of the interaction matrix element between the ground band and the aligned $(vi_{13/2})^2$ band [30].

In comparison to the first yrast band crossings caused by the $vi_{13/2}$ neutron pair alignments in ^{158,160,162,164}Yb isotopes, the second yrast band crossing systematics are little complicated. The ^{158,160,162}Yb isotopes show a sharp upbend around the rotational frequencies 0.36–0.46 MeV, while the ^{164}Yb displays a gradual increase in alignment. In Refs. [10,27], the second yrast band crossings observed at rotational frequency 0.42 MeV in ^{160}Yb [10] and rotational frequency 0.46 MeV in ^{162}Yb [27], respectively, have been suggested to correspond to the alignment of a pair of $h_{11/2}$ protons, which was also predicted by the theoretical calculations [31]. In the earlier studies for the ^{158}Yb [32,33], the high-spin states with spin $= 26^+$–36^+ in ^{158}Yb were found to exhibit a nearly vibrational excitation pattern, which was interpreted in terms of a gradual transition toward oblate shape and a band termination occurring at spin $= 36^+$. In the following study by Patel *et al.* [18], the high-spin states of ^{158}Yb was reinterpreted. On the basis of the systematics and CSM calculations, especially with a knowledge of high-spin structures in neighboring ^{156,158}Er, where clear band terminations were observed, it was suggested that the second upbend around rotational frequency 0.36 MeV in ^{158}Yb is also caused by a pair of $h_{11/2}$ proton alignment, while a pair of $h_{9/2}$ neutron alignment may be responsible for third upbend occurring around rotational frequency 0.39 MeV. The ^{158}Yb will remain rather collective in the yrast band up to at least spin 34^+ [18]. One interesting observation in Fig. 5 is the rotational frequencies at which the $h_{11/2}$ protons align in the ^{158,160,162}Yb isotopes increase with increasing neutron number. This shift may be related to a change in their nuclear deformations, which will be discussed later.

It has been suggested that a pair of $h_{9/2}$ neutron alignment might be responsible for the observed gradual increase in alignment in ^{164}Yb, while the second $i_{13/2}$ neutron pair alignment will occur at a little higher rotational frequency [28]. CSM calculations [18] showed that $h_{9/2}$ neutron configuration is strongly triaxial and oblate driving, whereas the $h_{11/2}$ proton configuration and the $i_{13/2}$ neutron configuration are not. Thus, if this pattern happens, it implies that the ^{164}Yb may undergo a shape transition from prolate to oblate and band termination. But the regular yrast band structure and lack of any branching at higher spin states in ^{164}Yb indicate that this pattern may not be true. In the neighboring ^{164,166}Hf, similar

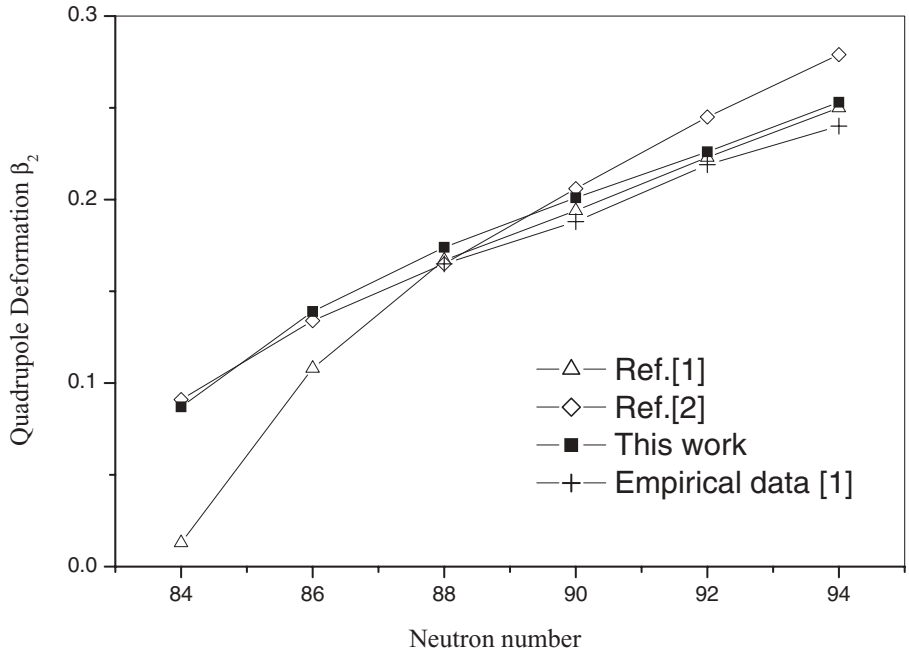

FIG. 8. The quadrupole deformation parameters β_2 for the ground-state of even-A ^{154,156,158,160,162,164}Yb isotopes by TRS calculations. The available empirical values deduced from $BE(2)$ measurements and two theoretical calculations using the macroscopic-microscopic shell correction method and RMF theory are also shown for comparison.

high-spin behaviors at the second band crossing region were also observed [34]. The alignment in ^{166}Hf was explained in term of the decoupling of the second $i_{13/2}$ neutron pair. Based on the CSM calculations and empirical systematics, we believe that the second band crossing involves a second pair of aligning $i_{13/2}$ neutrons as well as an $h_{11/2}$ proton pair resulting in the smooth upbend observed in ^{164}Yb.

Here, to get a further systematic understanding of the effects of alignments on the structure evolutions in even-A Yb isotopes, cranked Woods-Saxon-Strutinsky calculations for these nuclei have been performed by means of total-Routhian-surface (TRS) methods in a three-dimensional deformation space (β_2, γ, β_4) [35,36]. At a given frequency, the deformation of a state is determined by minimizing the calculated TRS. The theoretical values of the quadrupole deformation parameters β_2 for the ground states of even-A $^{154-164}$Yb isotopes are displayed in Fig. 8, in comparison with other theoretical calculations [12,13] and the empirical data [12] obtained from experimental $BE(2)$ values. The TRS results reproduce the empirical values very well, which show an increasingly prolate shape with an increase in neutron number, and are also consistent with the other two calculations using the macroscopic-microscopic shell correction method [12] and RMF theory [13], respectively.

Our TRS calculations predict that the first band crossings in the yrast bands of even-A $^{158-164}$Yb isotopes caused by an $i_{13/2}$ neutron pair alignment occur around rotational frequencies 0.25 MeV and an $h_{11/2}$ proton pair alignment occurs first in ^{156}Yb in the vicinity of rotational frequency 0.25–0.30 MeV. These theoretical results are in good agreement with the experimental values. The calculated crossing frequencies for the first $h_{11/2}$ proton-pair alignments are 0.33, 0.42, and 0.50 MeV for ^{158,160,162}Yb, respectively, which also well reproduce the experimental values. At these crossing frequency regions caused by the first $h_{11/2}$ proton pair alignment, the calculated quadrupole deformation values for ^{156,158,160,162}Yb are 0.145, 0.181, 0.204, and 0.232, respectively, while the calculated γ deformation values lie between 0° and 10°. CSM calculations by Riley *et al.* [37] already found that crossing frequency of the $h_{11/2}$ proton-pair alignment is not very

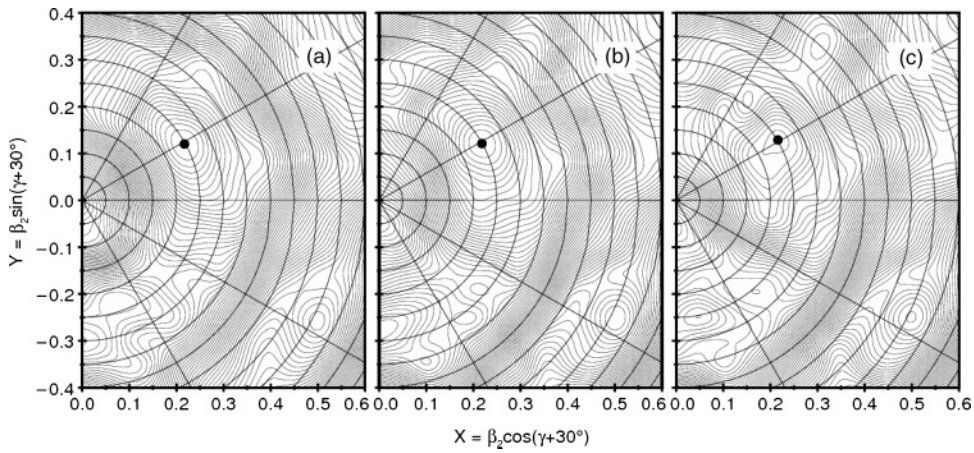

FIG. 9. TRS calculations for the yrast sequence in ^{164}Yb. The energy contours are at 200 keV intervals. The deformation parameters for the individual minima are (a) $\hbar\omega = 0.35$ MeV, $\beta_2 = 0.248$, $\gamma = -1.0°$, and $\beta_4 = -0.008$; (b) $\hbar\omega = 0.45$ MeV, $\beta_2 = 0.250$, $\gamma = -0.9°$, and $\beta_4 = -0.007$; (c) $\hbar\omega = 0.55$ MeV, $\beta_2 = 0.252$, $\gamma = 0.8°$, and $\beta_4 = -0.015$.

sensitive to the γ deformation values around this range. Thus, the variation in the crossing frequencies for the $h_{11/2}$ proton pair alignments observed in ^{156,158,160,162}Yb might be assumed to be predominantly due to variation in the quadrupole deformation β_2. According to our TRS calculations, the second $i_{13/2}$ neutron pair alignment in ^{164}Yb occurs around the rotational frequency 0.50–0.55 MeV, which is almost simultaneous with the first $h_{11/2}$ proton pair alignment. It further confirms the cause of the smooth upbend observed in ^{164}Yb. Around the band crossing region caused by this second $i_{13/2}$ neutron pair alignment and the first $h_{11/2}$ proton pair alignment rather than by the strongly triaxial driving $h_{9/2}$ neutron pair alignment, the TRS results, as shown in Fig. 9, indicate that ^{164}Yb keeps a fairly stably prolate deformation with very small triaxiality variances.

At higher rotational frequencies above the alignment frequencies of the $h_{11/2}$ proton pair in ^{156,158,160,162,164}Yb, our TRS results predict a shape change with sizable alignments occurring: from prolate ($\gamma = 0^\circ$), via triaxial, to oblate ($\gamma = 60^\circ$). The critical rotational frequency of this shape evolution increases with increasing neutron number. This shape change was also predicted by the theoretical calculations within the cranking approximation using the generalized Strutinsky methods [17] and has been observed in some experimental studies. For example, the spectroscopy studies of ^{160}Yb by Byrski *et al.* [10] indicated that the nuclear shape will arrive $\gamma = 60^\circ$ around spin 36^+ and band termination occurs. This process will produce a pronounced reduction in the collcetivity, which was observed by the following measurements of lifetimes of ^{160}Yb yrast states at high rotational frequencies [38]. A recent observation of a high-spin rotational band in ^{160}Yb [39] suggested a new shape minimum with strongly deformed triaxial configurations at high-spin states. Furthermore, according to the theoretical calculations [17], the superdeformed configurations will occur around spins 30–40$\hbar$ in ^{156,158}Yb, while the superdeformation exists at spin $\sim 70\hbar$ in ^{160}Yb. To find the superdeformed bands predicted in ^{156,158,160}Yb and get deeper understanding of all these rich structure phenomena at large angular momenta observed in even-A Yb isotopes, more experimental and theoretical works are needed.

IV. SUMMARY

High-spin states in ^{156}Yb have been populated in the ^{144}Sm(^{16}O,4n)^{156}Yb fusion-evaporation reaction at beam energy 102 MeV. Based on the γ-γ coincidence relationships, intensity balances and DCO analyses, the level scheme of ^{156}Yb has been constructed and discussed in comparison with similar structures observed in the neighboring $N = 86$ isotones. Several parallel cascades above the 25^- state in ^{156}Yb were found in the present work. This pattern may involve the excitation from nucleon in the $Z = 64$, $N = 82$ core. The characteristic of alignment plot and E-GOS curve for the positive-parity yrast sequences in ^{156}Yb suggest that this nucleus may undergo an evolution from quasivibrational to quasirotational structure with increasing angular momentum. Our TRS calculations indicate that the alignment of a high-j intruder $h_{11/2}$ proton pair may be the origin of this structure evolution.

Based on a systematic comparison of the behaviors of even-A ^{156,158,160,162,164}Yb isotopes at large angular momenta, the structure evolutions induced by the increase in angular momentum, as well as by the change in neutron numbers, in these even-A Yb isotopes have been discussed. The almost constant crossing frequencies around 0.27 MeV for the first band crossings observed in the yrast bands of ^{158,160,162,164}Yb can be ascribed to the compensation between the decrease in the neutron pair gap and the decrease in the alignment of the $i_{13/2}$ neutron pair with increasing neutron number. The alignments of a pair of $h_{11/2}$ protons have been suggested to be responsible for the sharp upbends occurring around the rotational frequencies 0.36–0.46 MeV in ^{158,160,162}Yb. Our TRS calculations for the second yrast band crossings give good agreement with the experimental values. The TRS results also indicate that the variation in the crossing frequencies for the first $h_{11/2}$ proton pair alignments in ^{156,158,160,162}Yb might be mainly due to variation in the quadrupole deformation β_2. The gradual increase in alignment in ^{164}Yb has been suggested to correspond to a pair of $h_{9/2}$ neutron alignment. Based on the systematic comparison with the similar pattern observed in the neighboring Hf isotopes and our TRS calculations, the second $i_{13/2}$ neutron pair alignment, also including the $h_{11/2}$ proton pair alignment, rather than the strongly triaxial driving $h_{9/2}$ neutron pair alignment may be responsible for the smooth upbend observed in ^{164}Yb. The TRS results also show that ^{164}Yb will keep a fairly stably prolate deformation with very small triaxiality variances around this second crossing frequency region. At higher rotational frequencies for the ^{156,158,160,162,164}Yb, Our TRS results predict a shape change with sizable alignments occurring: from prolate ($\gamma = 0^\circ$), via triaxial, to oblate ($\gamma = 60^\circ$), which has been observed in the experimental studies for ^{160}Yb.

ACKNOWLEDGMENTS

This work is support by the Natural Science Foundation of China under Grant Nos. 10405001, 10775005, 10735010, 10605001, J0730316 and, the Chinese Major State Basic Research Development Program under Grant No. 2007CB815002. The authors wish to thank Prof. G. J. Xu and Q. W. Fan for making the target and the staffs in the tandem accelerator laboratory at the China Institute of Atomic Energy (CIAE), Beijing.

[1] C. Baktash, E. der Mateosian, O. C. Kistner, and A. W. Sunyar, Phys. Rev. Lett. **42**, 637 (1979).

[2] C. J. Lister, D. Horn, C. Baktash, E. der Mateosian, O. C. Kistner, and A. W. Sunyar, Phys. Rev. C **23**, 2078 (1981).

[3] K. Y. Ding, J. A. Cizewski, D. Seweryniak, H. Amro, M. P. Carpenter, C. N. Davids, N. Fotiades, R. V. F. Janssens, T. Lauritsen, C. J. Lister, D. Nisius, P. Reiter, J. Uusitalo, I. Wiedenhover, and A. O. Macchiavelli, Phys. Rev. C **62**, 034316 (2000).

[4] A. Keenan, R. D. Page, J. Simpson, N. Amzal, J. F. C. Cocks, D. M. Cullen, P. T. Greenlees, S. L. King, K. Helariutta, P. Jones, D. T. Joss, R. Julin, S. Juutinen, H. Kankaanpaa, P. Kuusiniemi, M. Leino, M. Muikku, A. Savelius, M. B. Smith, and M. J. Taylor, Phys. Rev. C **63**, 064309 (2001).

[5] J. Pedersen, B. B. Back, F. M. Bernthal, S. Bjørnholm, J. Borggreen, O. Christensen, F. Folkmann, B. Herskind, T. L. Khoo, M. Neiman, F. Pühlhofer, and G. Sletten, Phys. Rev. Lett. **39**, 990 (1977).

[6] J. Borggreen, S. Bjornholm, O. Christensen, A. Del Zoppo, B. Herskind, J. Pedersen, G. Sletten, F. Folkmann, and R. S. Simon, Z. Phys. A **294**, 113 (1980).

[7] M. A. Bentley, A. Alderson, G. C. Ball, H. W. Cranmer-Gordon, P. Fallon, B. Fant, P. D. Forsyth, B. Herskind, D. Howe, C. A. Kalfas, A. R. Mokhtar, J. D. Morrison, A. H. Nelson, B. M. Nyako, K. Schiffer, J. F. Sharpey-Schafer, J. Simpson, G. Sletten, and P. J. Twin, J. Phys. G: Nucl. Part. Phys. **17**, 481 (1991).

[8] K. Lagergren, B. Cederwall, T. Bäck, R. Wyss, E. Ideguchi, A. Johnson, A. Ataç, A. Axelsson, F. Azaiez, A. Bracco, J. Cederkäll, Z. Dombŕdi, C. Fahlander, A. Gadea, B. Million, C. M. Petrache, C. Rossi-Alvarez, J. A. Sampson, D. Sohler, and M. Weiszflog, Phys. Rev. Lett. **87**, 022502 (2001).

[9] F. S. Stephens, M. A. Deleplanque, R. M. Diamond, A. O. Macchiavelli, and J. E. Draper, Phys. Rev. Lett. **54**, 2584 (1985).

[10] T. Byrski, F. A. Beck, J. C. Merdinger, A. Nourreddine, H. W. Cranmer-Gordon, D. V. Elenkov, P. D. Forsyth, D. Howe, M. A. Riley, J. F. Sharpey-Schafer, J. Simpson, J. Dudek, and W. Nazarewicz, Nucl. Phys. **A474**, 193 (1987).

[11] M. A. Riley, T. B. Brown, N. R. Johnson, Y. A. Akovali, C. Baktash, M. L. Halbert, D. C. Hensley, I. Y. Lee, F. K. McGowan, A. Virtanen, M. E. Whitley, J. Simpson, L. Chaturvedi, L. H. Courtney, V. P. Janzen, L. L. Riedinger, and T. Bengtsson, Phys. Rev. C **51**, 1234 (1995).

[12] W. Nazarewicz, M. A. Riley, and J. D. Garrett, Nucl. Phys. **A512**, 61 (1990).

[13] G. A. Lalazissisa, M. M. Sharmab, and P. Ring, Nucl. Phys. **A597**, 35 (1996).

[14] T. Niksic, D. Vretenar, G. A. Lalazissis, and P. Ring, Phys. Rev. C **69**, 047301 (2004).

[15] K. Neergard and P. Vogel, Nucl. Phys. **A145**, 33 (1970).

[16] A. Faessler and M. Ploszajczak, Z. Phys. A **295**, 87 (1980).

[17] J. Dudek and W. Nazarewicz, Phys. Rev. C **31**, 298 (1985).

[18] S. B. Patel, F. S. Stephens, J. C. Bacelar, E. M. Beck, M. A. Deleplanque, R. M. Diamond, and J. E. Draper, Phys. Rev. Lett. **57**, 62 (1986).

[19] D. C. Radford, Nucl. Instrum. Methods Phys. Res. A **361**, 297 (1995).

[20] C. Baktash, *in Proceedings of the Conference on High Angular Momentum Properties of Nuclei, Oak Ridge, Tennessee* (Harwood Academic, New York, 1983), p. 207.

[21] B. M. Nyako, J. Simpson, P. J. Twin, D. Howe, P. D. Forsyth, and J. F. Sharpey-Schafer, Phys. Rev. Lett. **56**, 2680 (1986).

[22] C. Schuck, M. A. Deleplanque, R. M. Diamond, F. S. Stephens, and J. Dudek, Nucl. Phys. **A496**, 385 (1989).

[23] L. Nguyen, H. Sergolle, P. Aguer, G. Auger, G. Bastin, T. Lonnroth, J. P. Thibaud, and L. Thome, Z. Phys. A **309**, 207 (1983).

[24] M. H. Rafailovich, O. C. Kistner, A. W. Sunyar, S. Vajda, and G. D. Sprouse, Phys. Rev. C **30**, 169 (1984).

[25] P. H. Regan, C. W. Beausang, N. V. Zamfir, R. F. Casten, Jing-ye Zhang, A. D. Yamamoto, M. A. Caprio, G. Gurdal, A. A. Hecht, C. Hutter, R. Krucken, S. D. Langdown, D. A. Meyer, and J. J. Ressler, Phys. Rev. Lett. **90**, 152502 (2003).

[26] L. L. Riedinger, O. Andersen, S. Frauendorf, J. D. Garrett, J. J. Gaardhoje, G. B. Hagemann, B. Herskind, B. Makovetzky, J. C. Waddington, M. Guttormsen, and P. O. Tjom, Phys. Rev. Lett. **44**, 568 (1980).

[27] J. N. Mo, S. Sergiwa, R. Chapman, J. C. Lisle, E. Paul, and J. C. Willmott, J. Hattula, M. Jaaskelwinen, J. Simpson , P. M. Walker, J. D. Garrett, G. B. Hagemann, B. Herskind, M. A. Riley, and G. Sletten, Nucl. Phys. **A472**, 295 (1987).

[28] A. Nordlund, R. Bengtsson, P. Ekstrom, M. Bergstrom, A. Brockstedt, H. Carlsson, H. Ryde, Y. Sun, A. Atac, G. B. Hagemann, B. Herskind, H. J. Jensen, J. Jongman, S. Leoni, A. Maj, J. Nyberg, and P. O. Tjom, Nucl. Phys. **A591**, 117 (1995).

[29] S. Jónsson, N. Roy, H. Ryde, W. Walu , J. Kownacki, J. D. Garrett, G. B. Hagemann, B. Herskind, R. Bengtsson, and S. Åberg, Nucl. Phys. **A449**, 537 (1986).

[30] R. Bengtsson and S. Frauendorf, Nucl. Phys. **A314**, 27 (1979).

[31] A. Faessler and M. PloszaIczak, Phys. Lett. **B76**, 1 (1978).

[32] C. Baktash, Y. Schutz, I. Y. Lee, F. K. McGowan, N. R. Johnson, M. L. Halbert, D. C. Hensley, M. P. Fewell, L. Courtney, A. J. Larabee, L. L. Riedinger, A. W. Sunyar, E. der Mateosian, O. C. Kistner, and D. G. Sarantites, Phys. Rev. Lett. **54**, 978 (1985).

[33] I. Ragnarsson, T. Bengtsson, W. Nazarewicz, J. Dudek, and G. A. Leander, Phys. Rev. Lett. **54**, 982 (1985).

[34] K. P. Blume, H. Hübel, M. Murzel, J. Recht, K. Theine, H. Kluge, A. Kuhnert, K. H. Maier, A. Maj, M. Guttormsen, and A. P. De Lima, Nucl. Phys. **A464**, 445 (1987).

[35] W. Satula, R. Wyss, and P. Magierski, Nucl. Phys. **A578**, 45 (1994).

[36] F. R. Xu, W. Satula, and R. Wyss, Nucl. Phys. **A669**, 418 (2000).

[37] M. A. Riley, J. Simpson, R. Aryaeinejad, J. R. Cresswell, P. D. Forsyth, D. Howe, P. J. Nolan, B. M. Nyakó, J. F. Sharpey-Schafer, P. J. Twin, J. Bacelar, J. D. Garrett, G. B. Hagemann, B. Herskind, and A. Holm, Phys. Lett. **B135**, 275 (1984).

[38] N. R. Johnson, F. K. McGowan, D. F. Winchell, C. Baktash, J. D. Garrett, I. Y. Lee, C. Wells, L. Chaturvedi, W. B. Gao, W. C. Ma, Pilotte , and C.-H. Yu, Phys. Rev. C **53**, 671 (1996).

[39] A. Aguilar, D. B. Campbell, K. Chandler, A. Pipidis, M. A. Riley, C. Teal, J. Simpson, D. J. Hartley, F. G. Kondev, R. M. Clark, M. Cromaz, P. Fallon, I. Y. Lee, A. O. Macchiavelli, and I. Ragnarsson, Phys. Rev. C **77**, 021302(R) (2008).